Encapsulation-enhanced genetic switches in lactobacilli

Marc Blanch-Asensio,[1,2], Varun Sai Tadimarri,[1,2], Roberto Martinez,[1,2], Gurvinder Singh Dahiya[3], Rahmi Lale,[3, 4] and Shrikrishnan Sankaran[1]

[1] INM - Leibniz Institute for New Materials, Saarland University, Campus D2 2, 66123 Saarbrücken, Germany

[2] Saarland University, 66123 Saarbrücken, Germany

[3] Syngens AS, 7089 Norway

[4] Department of Biotechnology and Food Science, Faculty of Natural Sciences, Norwegian University of Science and Technology, Trondheim, N-7491 Norway

*E-mail: Shrikrishnan.sankaran@leibniz-inm.de

ABSTRACT

Lactiplantibacillus plantarum, a versatile member of the lactobacillus family, is widely recognized for its potential in healthcare, food production, and environmental biotechnology. Despite its inherent advantages and demonstrated potential as microbial chassis for biotechnological applications, its broader utility is constrained by a limited genetic toolbox, particularly the lack of robust genetic switches for inducible gene expression. Addressing this gap, we report the development of a novel genetic switch for *L. plantarum* based on a strong bacteriophage-derived promoter and the food-grade inducer, cumate. The dynamic range and temporal profile of this switch exhibits interesting temperature and growth phase dependence that influence its leakiness and induced protein production levels. In the process of identifying ways to overcome both dependencies, we discovered that encapsulation of *L. plantarum* in alginate seemingly traps them in a growth-phase that maximizes the performance of the switch. For the first time, we show how a material-oriented strategy can be leveraged to improve an engineered gene regulation function in bacteria. Furthermore, this engineered living material approach is promising for developing *L. plantarum* towards advanced applications in biotechnology, pharmaceutics, and living therapeutics.

Keywords: Engineered living materials, *L. plantarum*, genetic switch, induction, PEARLs, micro-PEARLs.

INTRODUCTION

Lactobacilli are highly valued for their diverse applications across healthcare, food production, and environmental remediation (Giraffa, Chanishvili et al. 2010, Monachese, Burton Jeremy et al. 2012, Zhang, Lv et al. 2018). Among their notable advantages is their use in fermented foods and their ability to modulate gut microbiota, lower cholesterol, and attenuate inflammatory diseases (Santos Rocha, Lakhdari et al. 2012, Wang, Zhang et al. 2012). These characteristics highlight their potential as microbial chassis in diverse applications (Zhang, Niu et al.) Building on their inherent benefits, there has been growing interest in harnessing lactobacilli through genetic engineering for advanced biotechnological applications with the highest number of reports based on the species *Lactiplantibacillus* plantarum (Blanch-Asensio, Dey et al. 2024). For example, engineered lactobacilli have been modified to produce recombinant proteins for pharmaceutical applications, including vaccines and mucosal therapeutics (Scheppler, Vogel et al. 2002, Pan, Liu et al. 2021).

However, the applicability of lactobacilli as living therapeutics is hindered by their limited genetic toolbox. In the last decades, progress has been made concerning finding natural or engineered promoters to drive high levels of gene expression in *L. plantarum*. (Rud, Jensen et al. 2006, Peirotén and Landete 2020, Meng, Yuan et al. 2021). Nevertheless, lactobacilli still lack high-performance genetic parts like strong promoters, effective repressors, and reliable genetic switches for inducible gene expression compared to model bacteria such as *E. coli* (Blanch-Asensio, Dey et al. 2024). This gap has slowed the development of advanced genetic circuits needed for more precise control of gene expression. Reliable genetic switches have been particularly elusive to create. A few studies report expression systems such as xylose- or lactose-genetic switches but the fold changes upon induction are relatively poor in these reported cases (<10x) (Heiss, Hörmann et al. 2016). Bile-induced promoters have also been explored in lactobacilli, but their induction relies on intestinal conditions, which can restrict their applicability (Martínez-Fernández, Bravo et al. 2019). The most reliable and widely used switch is the pSIP system, which has been used to control the production of a wide range of proteins, including different enzymes and antigens (Sørvig, Mathiesen et al. 2005, Halbmayr, Mathiesen et al. 2008, Nguyen, Nguyen et al. 2011, Karlskås, Maudal et al. 2014, Yang, Li et al. 2018). Nevertheless, this switch is based on a two-component system, which limits its portability and adaptability, and relies on a peptide as an inducer, making it relatively cost-intensive.

Genetic switches are vital for the genetic programmability of an organism since they allow temporal control over gene expression (Brautaset, Lale et al. 2009, Meyer, Segall-Shapiro et al. 2019). In terms of recombinant protein production for biotechnology or pharmaceutic applications, this enables a separation between growth and production

phases, which can enhance productivity and reduce metabolic burden (Mao, Zhang et al. 2024). For living therapeutic or bioremediation applications, genetic switches enable biosensing functions or remote activation of desired responses like protein secretion (Yoon, Seo et al. 2024). However, inducible genetic switches in lactobacilli are plagued by limitations such as leaky expression or limited dynamic range, for which underlying reasons and reliable solutions are not known or reported in the literature.

Our recent studies have expanded the genetic programmability of *L. plantarum* by developing a high-performance promoter-repressor system derived from bacteriophages with the potential to aid the development of reliable genetic switches (Blanch-Asensio, Tadimarri et al. 2024). Moreover, towards the applicability of such genetically engineered lactobacilli, we encapsulated them in core-shell alginate hydrogels to create the Protein Eluting Alginate with Recombinant Lactobacilli (PEARL) format (Tadimarri, Blanch-Asensio et al. 2025). These engineered living materials (ELMs) provided benefits such as containment of engineered bacteria, sustained protein release, and reduced metabolic toxicity for at least two weeks. Moreover, it stabilized the protein release profile of the engineered bacteria when compared to non-encapsulated bacterial cultures. These results suggested that the PEARL format influenced the metabolism of the encapsulated bacteria and could probably enhance the performance of engineered *L. plantarum*.

Thus, in this study, we build upon these advances to create a novel genetic switch for *L. plantarum* that responds to a food-grade inducer molecule, cumate (Meyer, Segall-Shapiro et al. 2019). We uncover interesting temperature and growth phase dependent phenomena that influence leakiness and induced expression levels. More interestingly, by encapsulating these engineered strains in the PEARL format, we discovered that the bacteria remain trapped in a growth phase that favorably minimizes leaky expression and maintains high levels of protein production upon induction. We further demonstrate the possibility of extending this approach to another highly leaky genetic switch, induced by vanillate, and leverage this capability to develop dual-switchable PEARLs. Finally, we show that this leakiness-suppressing-effect is sustained even when the PEARLs are miniaturized by an order of magnitude. These interesting results suggest that this encapsulation strategy stabilizes genetic switches in *L. plantarum,* and this ELM approach might be promising for further development of gene regulation in lactobacilli.

EXPERIMENTAL SECTION

Strains, media and plasmid vector

L. plantarum WCFS1 was used in this study. The strain was grown in De Man, Rogosa and Sharpe (MRS) media (Carl Roth GmbH, Germany, art. no. X924.1). The strain was incubated at either 30° or 37°C (indicated in each case), and 250 revolutions per minute (rpm). The media of the engineered strains were supplemented with 10 µL/mL of erythromycin (Carl Roth GmbH, Germany, art. no. 4166.2). For the cloning of all the plasmids, NEB DH5-α competent *E. coli* cells were used (New England Biolabs GmbH, Germany,Art. No. C2987). Engineered *E. coli* was grown in Luria-Bertani (LB) media (Carl Roth GmbH, Art. No. X968.1) supplemented with 200 µg/mL of erythromycin at 37°C and 250 rpm shaking conditions. The pLp_3050sNuc plasmid (Addgene plasmid # 122030) was the backbone vector for all the plasmids used in this work.

Molecular cloning reagents

Primers were synthesized by Eurofins Genomics GmbH (Köln, Germany). All the primers used in this study are listed in **Table S1**. Synthetic gene fragments were ordered as eBlocks from Integrated DNA Technologies (IDT) (Coralville, USA). The codon optimization tool of IDT was used to codon-optimize the eBlocks (selecting the option for *Lactobacillus acidophilus*). All the eBlocks used in this study are listed in **Figure S0**. For the *polymerase* chain reaction (PCR), Q5 High Fidelity 2X Master Mix (NEB GmbH, Germany, No. M0492S) was used. 1 kb Plus DNA Ladder (Catalog Number 10787018) was purchased from ThermoFisher Scientific (Germany) and used as a reference in gel electrophoresis. The Wizard® SV Gel and PCR Clean-Up system (Promega GmbH, Germany, Art. No. A9282) was used to purify the PCR products. DNA assembly was performed using the HiFi Assembly Master Mix (NEB GmbH, Germany, Art. No. E5520S). The Qiagen GmbH (Hilden, Germany) plasmid extraction kit was used to lyse and extract the plasmids from E. coli DH5α.

Plasmid construction

The eBlocks were designed with compatible ends (20 base-pair overhangs) to the backbone vector. Each eBlock was resuspended with 20 µL of previously autoclaved Milli-Q water and used directly in the HiFi assembly reaction following the manufacturer's protocol. Right after, the assembled products were transformed into NEB DH5-α *E. coli* competent cells following the manufacturer's heat shock protocol except for the NucA cloning, where bacteria were grown at 28°C instead of 37°C. Plasmids were extracted

from *E. coli* DH5-α cells and used for transforming *L. plantarum* WCFS1 after sequence verification by Sanger sequencing (Eurofins Genomics GmbH (Köln, Germany)). All eBlock sequences are shown in **Figure S0**.

L. plantarum WCFS1 competent cell preparation and DNA transformation

Prior to electroporation, L. plantarum WCSF1 competent cells were prepared as described in (Blanch-Asensio, Dey et al. 2023). DNA transformation was done by electroporation, following the procedure described in (Blanch-Asensio, Dey et al. 2023).

Gene expression switches induction

Vanillic acid (vanillate) and 4-isopropylbenzoicacid (cumate) were purchased at Sigma Aldrich (Catalog number H36001 and 268402, respectively). Anhydrotetracycline (aTc) was purchased at Cayman Chemical (Item no. 10009542). All inducers were resuspended in pure ethanol. The concentrations used for inductions were: 50 μM of vanillate for the vanillate switch, 200 nM of aTc for the aTc switch, and 0.1 to 100 μM (indicated in each experiment) of cumate for the cumate switch. The induction time is indicated in each experiment. The pSIP system induction was done using the IP673 peptide (GeneCust, Boyes, France), to a final concentration of 100 ng/mL.

Flow cytometry analysis

Engineered *L. plantarum* WCSF1 were grown in 4 mL of MRS media supplemented with 10 μg/mL erythromycin at 37 °C and 250 rpm. The next day, bacteria were sub-cultured to an OD_{600nm} of 0.01 in 2 mL of MRS media supplemented with 10 μg/mL erythromycin and grown at 37 °C with shaking (250 rpm) for a period of 8 hours. For the induced conditions, inducers were added along with the erythromycin. After that, 1 mL of the bacterial cultures were pelleted down by centrifugation at 6000 rpm for 2 minutes. The supernatant was discarded carefully, and the pellets were resuspended in 1 mL of sterile Dulbecco's 1X PBS (DPBS). Finally, the mixtures were serially diluted by a 10^4 dilution factor, and 5,000 bacterial events were recorded for analysis using Guava easyCyte BG flow-cytometer (Luminex, USA). The fluorescence intensity of mCherry was measured using excitation by a green laser at 532 nm (100 mW) and the Orange-G detection channel 620/52 nm filter was used for signal analysis. The Luminex GuavaSoft 4.0 software for EasyCyte was used for the analysis and representation of data.

Microplate reader setup for induction levels assessment

Engineered *L. plantarum* WCSF1 were grown in 4 mL of MRS media supplemented with 10 µg/mL erythromycin at 37 °C and 250 rpm. After overnight growth, bacteria were sub-cultured to low OD_{600nm} (indicated in the results section) in MRS media supplemented with 10 µg/mL erythromycin. For the induced conditions, the inducers were added along with the erythromycin, and bacteria were incubated for a period of 5 to 8 hours (the exact time and cumate concentration are indicated in the results section). After that, bacterial pellets were resuspended in 1 mL of DPBS, 200 µL of the mixture were transferred to a UV STAR Flat Bottom 96 well microtiter plate (Greiner BioOne GmbH, Germany). The microplate reader Infinite 200 Pro (Tecan Deutschland GmbH, Germany) was used to quantify the levels of fluorescence. The mCherry fluorescence intensity was measured using the excitation/emission values: Ex_{λ} / Em_{λ} = 587 nm/625 nm. The fluorescence values were normalized with the OD_{600nm} of the mixtures (quantified by measuring the absorbance at 600 nm) to calculate the Relative Fluorescence Units (RFU) (Fluorescence/OD_{600nm}). In all cases, the RFU values for *L. plantarum* WCFS1 carrying an empty vector (a plasmid based on the origin and the antibiotic resistance) were used as blank. The setting for the microplate reader were as follows: the Z-position was set at 19000 µm, the gain settings at 80-100 (indicated in the results section), and the readings were taken from the top.

Microplate reader kinetics setup for induction assessment

Engineered *L. plantarum* WCSF1 were grown 4 mL of MRS media supplemented with 10 µg/mL erythromycin at 37 °C and 250 rpm. After overnight growth, bacteria were sub-cultured to low OD_{600nm} and incubated at 37 °C and 250 rpm. After 8 hours of growth, bacteria were again diluted to an OD_{600nm} of 0.01 with MRS supplemented with 10 µg/mL erythromycin. For the induced conditions, 5 µM of cumate, 50 µM of vanillate or 100 ng/mL of IP673 peptide were added for induction. Next, bacteria were transferred to a 96-well plate, and a kinetic cycle was set at 37°C or 30°C for up to 16 hours (indicated in the results section). Fluorescence intensity and OD_{600nm} values were taken every 30 minutes. RFU values were calculated as described in the previous section.

NucA Assay (in DNase media with Methyl green)

Qualitative Assay:

Engineered *L. plantarum* WCSF1 were grown overnight in MRS media supplemented with 10 µg/mL erythromycin at 37°C, 250 rpm. The next day, the OD_{600nm} was measured, and bacteria were subcultured in 4 mL of MRS media supplemented with 10 µg/mL erythromycin at an OD_{600nm} of 0.05 and incubated for approximately 5 hours at 30 or 37°C until OD_{600nm} was close to 1. For the included conditions, 5 µM of cumate was added during the subculturing. 5 hours later, 10 µL of the cultures were spotted on DNase agar (Altmann Analytik GmbH, Germany) supplemented with 10 µg/mL of erythromycin and incubated at 37°C for 40 hours. After this incubation, the BioRad Gel Documentation System was used to capture images of the DNase agar plates, and the fluorescence of the halo generated around the spotted area was measured using ImageJ (version 1.53k).

Quantitative Assay:

Engineered *L. plantarum* WCSF1 was grown as described in the qualitative assay section. When bacteria reached an OD_{600nm} of approximately 1, bacteria equivalent to OD_{600nm} of 0.1 were transferred to 1 mL of DNase media supplemented with 10 µg/mL erythromycin and incubated at 30 or 37ºC and 250 rpm shaking conditions for 24 hours. For the included conditions, 5 µM of cumate was added during the subculturing. The DNase media was obtained as described in (Tadimarri, Blanch-Asensio et al. 2025). After 24 hours, the cultures were centrifuged at 7000 rpm and 200 µL of the supernatants were added to the clear bottom 96-well microtiter plate. The samples were analyzed in the microplate reader Infinite 200 Pro was used to measure the fluorescence intensity of the supernatants (Exλ / Emλ = 633/668 nm). The Z-position was set at 19000 µm and the gain settings at 100. The NucA concentration was correlated and calculated using the standard curve at 24 hours described in (Tadimarri, Blanch-Asensio et al. 2025).

PEARLs fabrication and cumate-responsiveness

Fabrication

PEARLs were fabricated as described in (Tadimarri, Blanch-Asensio et al. 2025). In brief, 3 wt% alginate solution was prepared by dissolving alginate in sterile Milli-Q water, followed by autoclaving the solution for 15 minutes at 121°C. Equal amounts of 3 wt% alginate and *L. plantarum* WCSF1 were resuspended in LB media supplemented with 10 µg/mL erythromycin (approximately 10^8 cells per mL) were mixed and vortexed to obtain

the core solution (of 1.5 wt%). Equal amounts of 3 wt% alginate and sterile Milli-Q water were mixed to obtain the shell solution (of 1.5 wt%). 10 µL droplets of core solution were pipetted and dropped into a 5 wt% $CaCl_2$ solution (ionic crosslinker). The droplets were left to polymerize in the ionic crosslinker for 15 minutes. After that, the core beads were collected and washed thrice with sterile Milli-Q water. Alginate core beads were dipped into a 2-mL eppendorf with 1.5 wt% shell alginate solution and core bead with 25 µL of shell solution was pipetted and dropped into 5 wt% cross-linker solution. Core-shell PEARLs were left to polymerize in the cross-linker solution for 15 minutes before the induction experiments.

Cumate induction and quantification

PEARLs were transferred into a 96-well plate, and 200 µL of LB media supplemented with 10 µg/mL erythromycin were added. For the induced conditions, 100 µM of cumate or 50 µM of vanillate were added. Next, the microplate reader was used to track bacterial leakiness (bacterial growth as an increase in absorbance at 600 nm), and mCherry production (Ex/Em = 587/625 nm) for 24 to 70 hours depending on the experiments. Measurements were taken every 30 minutes. Manual gain was set at 100, Z-position at 19000 µm, temperature was 37 °C and integration time was 20 µs. The BioRad Gel Documentation System was also used to capture macroscopic images of the PEARLs after induction. Images were processed with ImageJ.

For the NucA experiments, 200 µL of DNase (supplemented with 10 µg/mL erythromycin) media without or with cumate (100 µM) was added. NucA secretion was measured by taking measurements at Ex/Em = 633/668nm and absorbance at 600 nm for 24 hours at 37°C, taking measurements every 30 minutes. Manual gain was set at 100, Z-position at 19000 µm and integration time was 20 µs. After 48 kinetic cycles (day 1), the DNase media was removed, and the wells were washed with 200 µL of sterile Milli-Q water. Next, 200 µL of fresh DNase (supplemented with 10 µg/mL erythromycin) media without or with cumate (100 µM) was added, and measurements were taken for 48 new kinetic cycles (day 2).

Micro-PEARLs fabrication, secretion assessment and cumate responsiveness

Fabrication

The core and shell solutions were prepared in the same compositions as prepared for PEARLs. 5 mL of core solution was filled in a 5 mL syringe and 20 mL of shell solution was filled in a 20 mL syringe. Micro-PEARLs were fabricated using the microencapsulator B-390 (Buchi, Switzerland). The autoclaved reaction vessel was arranged with 150 µm

nozzle (for core) and 300 µm nozzle (for shell). Syringes with core and shell alginate solutions were secured to the respective entry points of the aseptic reaction vessel. 200 mL of crosslinker solution (5 wt% CaCl2 solution) was introduced into the reaction vessel through the hose with filter (Sartorius, Germany). The microencapsulator device was switched on and voltage (1600 V), frequency (910 Hz), syringe pump for core (20 mL/second), syringe pump for shell (7 mL/second) and stirrer (40 %) were enabled. The micro-PEARLs with core and shell were dropped into the reaction vessel until the core solution ran out. The micro-PEARLs were left in the reaction vessel for up to 15 minutes for polymerization. The micro-PEARLs were collected in a sterile schott flask connected to the device through an efflux port at the bottom of reaction vessel. The micro-PEARLs were finally washed thrice with sterile Milli-Q water. The reaction vessel and the nozzles were cleaned by pumping sterile water and the device was autoclaved at 121 °C.

NucA secretion assessment

After the washes, the micro-PEARLs were collected with a sterile spatula and placed in the center of DNase agar (Altmann Analytik GmbH, Germany) plates supplemented with 10 µg/mL of erythromycin and incubated at 37°C for 5 days. The next day, the discoloration zone was captured using the BioRad Gel Documentation System. The images were processed using ImageJ.

Cumate induction

After three washes with sterile Milli-Q water, the micro-PEARLs were collected with a sterile spatula and placed in either 2-mL tubes or a 12-well plate. For the induction in the tubes, 1 mL of LB media supplemented with 10 µg/mL of erythromycin and 100 µM of cumate was added. Induction was performed for approximately 24 hours. After that, induction was assessed with the BioRad Gel Documentation System or the Keyence microscope (BZ-X800E). For induction in the plates, 500 µL of LB supplemented with 10 µg/mL of erythromycin and 100 µM of cumate was added per well. The plate was placed in the microplate reader and an increase in mCherry production (Ex/Em = 587/625 nm) was tracked for 19 hours approximately. The absorbance at 600 nm was also measured for normalization of the values. Measurements were taken every 30 minutes. Manual gain was set at 100, Z-position at 23000 µm and integration time was 20 µs.

Fluorescence Microscopy

The Keyence microscope (BZ-X800E) was used to perform microscopy of micro-PEARLs. After the induction, micro-PEARLs were transferred to a 12-well plate with glass bottom for better imaging. Multichannel images of micro-PEARLs were captured in 4X and 10X

(S plan fluor objective) magnification using the CH3 (red fluorescence) and CH4 (brightfield) channels. The images were processed and analyzed using ImageJ.

Statistical analysis

Statistical analysis was done using GraphPad Prism 7.0 software. Student's t-tests were used to determine statistically significant differences among the means of the groups. The differences among groups are indicated as: no statistically significant difference (ns), *p*-values <0.05 (*), *p*-values <0.01 (**), *p*-values <0.005 (***), *p*-values <0.001 (****).

RESULTS AND DISCUSSION

Developing a genetic switch in *L. plantarum*

To create a genetic switch in *L. plantarum*, we leveraged our previously discovered phage-derived strong constitute promoter, P_{tec}. We modified the promoter with operator sequences where can bind three switchable repressors from promising food-grade small-molecule inducible gene expression systems that were previously established in other bacteria - the anhydrotetracycline (aTc) system, proven to work in multiple bacteria such as *Escherichia coli*, *Vibrio cholerae* or *Streptococcus suis* (Lutz and Bujard 1997, Bina, Wong et al. 2014, Zhang, Zou et al. 2022), the cumate system, which functioned well in *Pseudomonas aeruginosa* and *Bacillus* subtilis (Seo and Schmidt-Dannert 2019, Klotz, Kaczmarczyk et al. 2023), and the vanillate system, which showed promising results in *E.* coli (Kunjapur and Prather 2019). Accordingly, the P_{tec} promoter was flanked by the corresponding operator sequences, one placed upstream and the other downstream of the promoter sequence (**Figure 1A, S1A**).

All three switches were designed with the same plasmid architecture, which harbored the P_{256} origin of replication and erythromycin resistance gene. The mCherry reporter gene was positioned downstream of the operator-flanked P_{tec} promoter, while the repressor for each genetic switch was placed under the control of the moderate-strength constitutive promoter P_{23} (Meng, Yuan et al. 2021) (**Figure 1A**). This was done to ensure that the repressor gene was continuously expressed, while mCherry expression could be switched ON and OFF upon the addition of the respective inducers (aTc, cumate and vanillate) (**Figure 1B**). Using flow cytometry, we assessed the responsiveness of each genetic switch to the given inducer after 8 hours of induction, seeking a candidate that strongly represses P_{tec} in the absence of the inducer and triggers strong protein production upon induction (**Figure 1C**). The aTc switch (P_{23}_tetR variant) showed nearly negligible leaky mCherry expression in the absence of the inducer but also very weak levels of expression upon induction with 200 nM of aTc (~3x fold change vs uninduced, **Figure S1B**). The cumate switch (P_{23}_cymR variant) was more promising, with low levels of leakiness when uninduced (similar to wild-type *L. plantarum* WCFS1) and significantly higher levels of mCherry expression upon induction with 100 µM of cumate (~27x fold change vs uninduced, **Figure S1B**). Finally, the vanillate switch (P_{23}_vanR variant) showed elevated levels of leakiness when uninduced and only slightly higher levels of expression with 50 µM vanillate (~2x fold change vs uninduced, **Figure S1B**). Overall, all three switches were responsive to their inducers, but since the cumate switch offered the best performance, we proceeded to further characterize and optimize this switch.

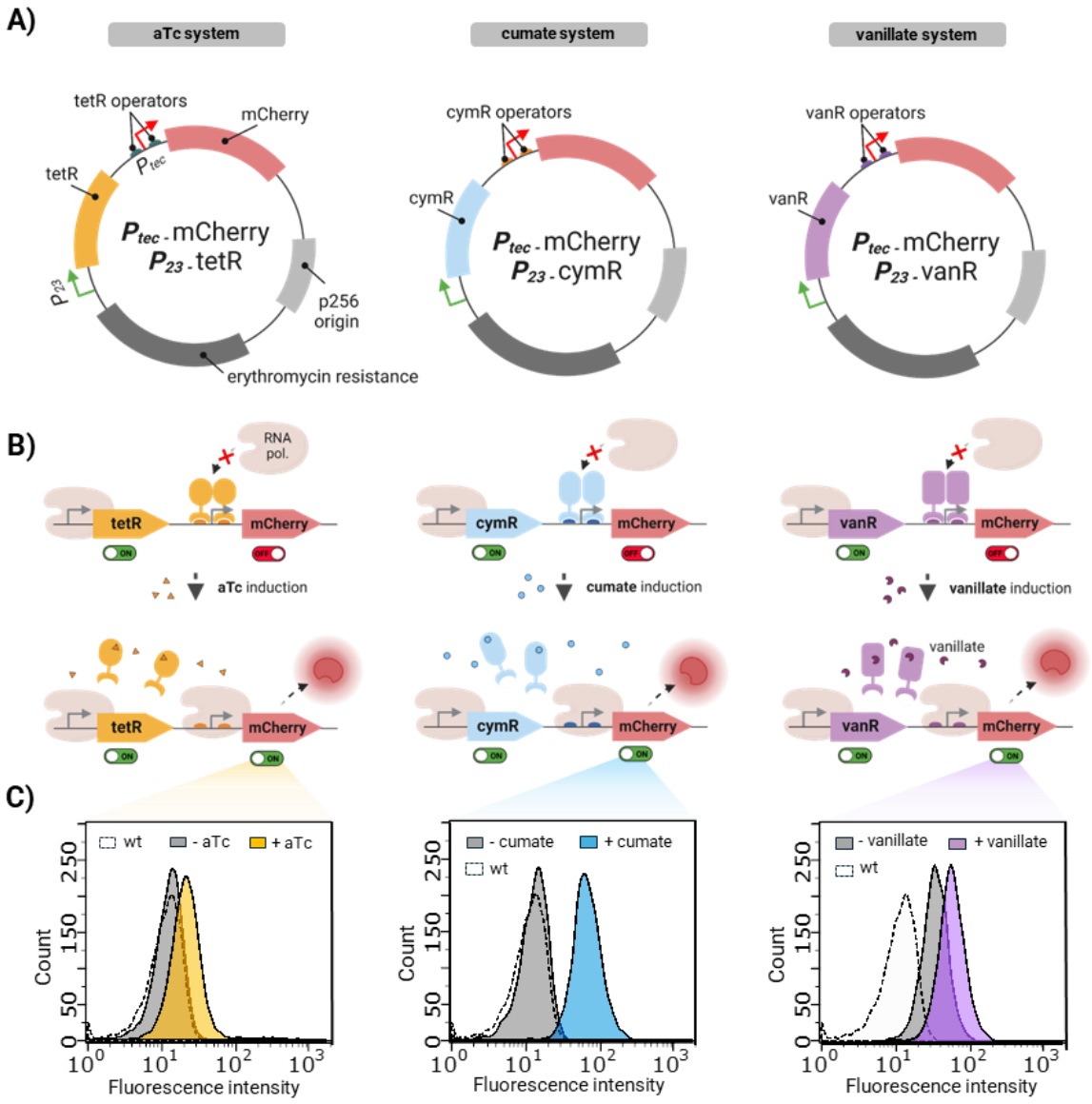

Figure 1: *Inducible genetic switches adapted for L. plantarum.* **A)** Plasmid maps for the aTc, cumate and vanillate switches. All the relevant genetic parts are depicted. **B)** Schemes showing the mode of action of the three inducible switches, and the expected outcome after the addition of the inducers. **C)** Histograms obtained by flow cytometry showing the red fluorescence intensity of the uninduced and induced states of each switch. For all, the fluorescence intensity of non-engineered *L. plantarum* is shown as reference for leakiness. Bacteria were subcultured to an OD_{600nm} of 0.05 and induced for 8 hours with 200 ng of aTc, 100 µM of cumate and 50 µM of vanillate, respectively.

Characterization of the cumate switch

First, we tested whether the genetic switch responds to cumate only due to inhibition of the CymR repressor. Hence, in the plasmid encoding this genetic switch, we removed the *cymR* gene and observed that bacteria constitutively produced as much mCherry as the variants with the repressor that were induced by cumate (100 μM). This not only proved that induction was mediated purely by the repressor but also suggested that cumate fully inactivated it (**Figure 2A**). By varying the inducer concentration, we further determined that 5 μM cumate was sufficient for maximal induction, below which expression levels dropped in a seemingly linear manner from 1 μM. This suggested the possibility to tune expression levels by varying the concentration of cumate in the culture (**Figure 2B**).

Nevertheless, we observed considerable leakiness in the switch, indicating that repression of the inducible gene is incomplete in the absence of cumate. We evaluated the leakiness of the switch by tracking increase in fluorescence without the inducer for 10 hours with cultures having different starting bacterial densities - OD_{600nm} of 0.3, 0.1 and 0.01. First, we noticed that leaky expression was not observed at the start of the experiment but was detectable only after at least 4 hours. This start of leaky expression was delayed by nearly 3 hours for the culture with an initial bacterial density of 0.01 OD_{600nm} (**Figure 2C**). This suggests that leaky expression can be detected only beyond a certain bacterial density. So, we studied the performance of the cumate switch over time with all three starting bacterial densities and correlated the data with kinetic measurements of bacterial growth. Interestingly, regardless of the initial bacterial density, the uninduced state started showing leaky expression once bacteria crossed a density of 0.8 OD_{600nm} (**Figure 2D**). This was in the late log-phase of growth, indicating that the operated P_{tec} promoter is repressed during the early and mid-log phases of growth.

We speculated that the leakiness could be associated with insufficient expression of the CymR repressor driven by the P_{23} promoter. Hence, we developed two additional variants by replacing P_{23} with P_{tlpA}, a stronger constitutive promoter (P_{tlpA}_cymR variant), and with the natural (non-operated) P_{tec} promoter (P_{tec}_cymR variant) (**Figure S2A**). Surprisingly, we observed similar trends as with the P_{23}_cymR variant (**Figure S2B**), with leakiness in the repression of the operated P_{tec} after 6-8 hours of growth (**Figure S2C** and **S2D**). This suggested that failure of the repressor was not due to its quantity in the cell, but some other factor associated with growth.

Since building a genetic switch based on two independent genes (the repressor gene and the inducible gene) did not address the leakiness problem, we redesigned the switch employing a feedback circuit where both the repressor (cymR) and gene of interest

(mCherry) are under the same operated P_{tec} promoter, hypothetically achieving gene expression only in the presence of cumate (**Figure 2E**). This feedback mechanism has been used in genetic switches in *E. coli* to improve the stability of the switch, but it has never been attempted in *L. plantarum* (Tan, Marguet et al. 2009, Daniel, Rubens et al. 2013). To ensure the production of both proteins, we included P_{23} ribosome-binding site between the STOP codon of the mCherry and the START codon of the cymR gene (**Figure 2F**). We termed this variant P_{tec}_cymR_P (polycistronic). This variant showed similar results concerning the leakiness of the switch, however, interestingly, the overall levels of production were higher (**Figure S2E**). To confirm the correlation between growth and leakiness, we repeated the kinetic studies at different starting bacterial densities (OD_{600nm} of 0.3, 0.1 and 0.01) with this variant. In this case, we observed leaky expression starting in the mid- to late-log phase with bacterial densities in the range of 0.6-0.8 OD_{600nm} (**Figure 2G**). When comparing all these constructs in terms of induced fold change over uninduced leaky expression, the P_{23}_cymR switch emerges as the superior system with a maximal fold change above 60x at 6 hours (**Figure S2F**). However, it is to be noted that fold changes for all switches vary over time being low at that start before induced expression starts, increasing to a maximum while leaky expression remains poor, and reducing again as leaky expression increases.

Next, we compared the performance of P_{23}_cymR (best fold change switch) and P_{tec}_cymR_P (highest production switch) with the most widely used genetic switch in *L. plantarum*, the pSIP system. This is a two-component system in which an inducer peptide (SppIP) binds a transmembrane receptor kinase, which in turn phosphorylates a response regulator that acts as an activator to initiate transcription from the P_{spp} promoter (Sørvig, Mathiesen et al. 2005). As expected, we observed clear differences between the performance of the cumate and the pSIP switches. Firstly, the pSIP switch showed negligible leakiness at all the assessed bacterial densities (0.3, 0.1 and 0.01). However, the overall levels of expression were significantly lower compared to the cumate switches (**Figure S3A**). For instance, after 12 hours of induction, mCherry production by the pSIP_409 system, was 8 to 17 times lower than that of the cumate switches (**Figure S3B**). Thus, the cumate switches based on the strong P_{tec} promoter outperformed the pSIP switch in terms of protein production but were also leakier. Nevertheless, these results showed that it is possible to repress the operated P_{tec} promoter during the early and mid-log phase of growth. Yet, finding a method to decrease the leakiness of the cumate switch and increase the uninduced-induced states fold change would add great value to the genetic programmability of *L. plantarum*.

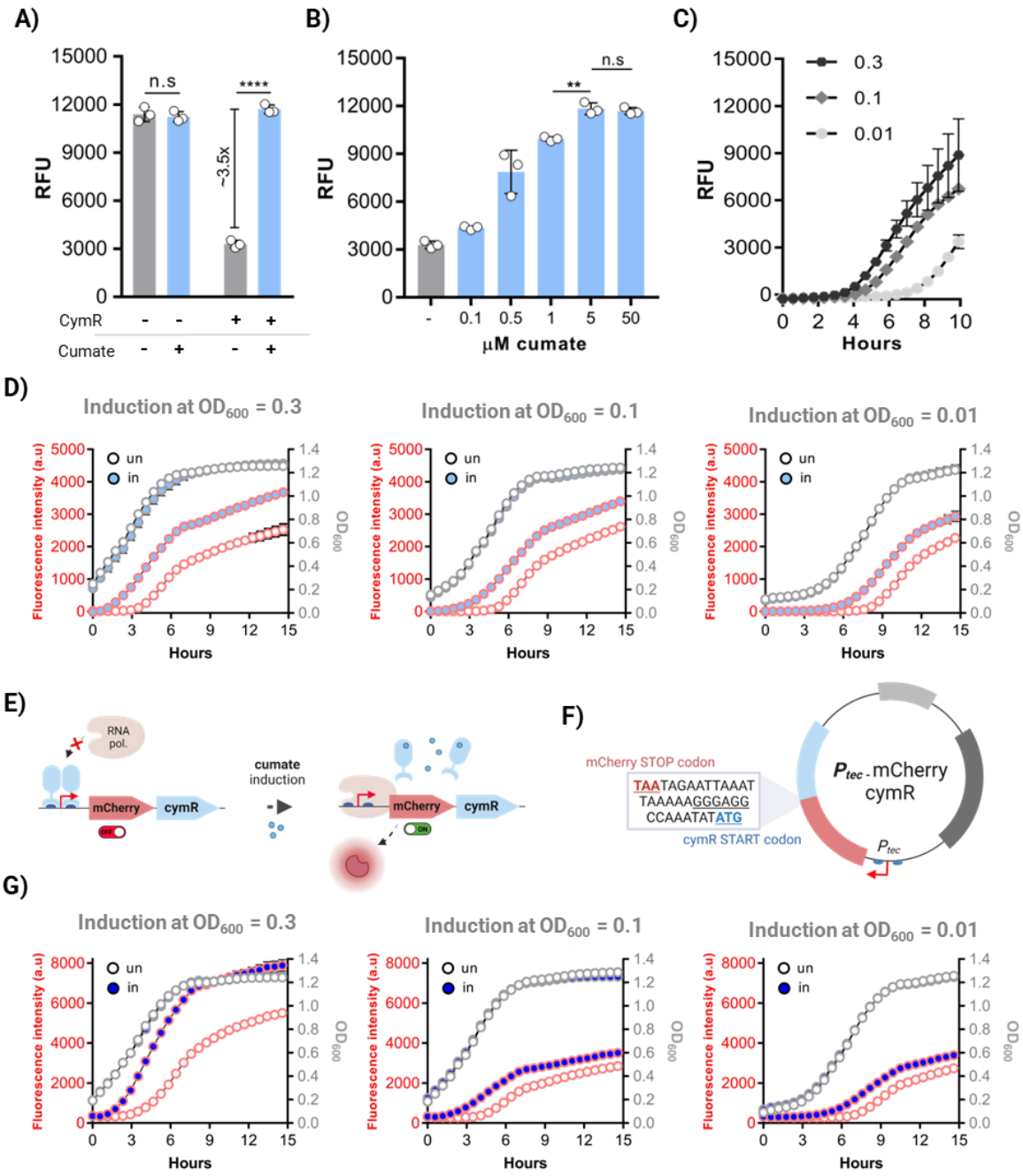

Figure 2: **Characterization of the cumate genetic switch**. **A)** RFU values after 8-h induction with 100 µM of cumate. When the CymR is not encoded in the plasmid (-), when CymR is encoded in the plasmid (+). When cumate is not added in the media (-). When cumate is added to the media (+) (n = 3, mean ± SD). **B)** RFU after inducing with different cumate concentrations for 8 hours (n = 3, mean ± SD). **C)** Growth-dependent leakiness (as RFU) of the cumate switch. **D)** Fluorescence intensity (left Y axis) and OD_{600nm} values (right Y axis) of the P_{23}_cymR variant when induced at different starting OD_{600nm} (0.3, 0.1 and 0.01) for 15 hours (n = 3, mean ± SD, gain = 85). **E**) Scheme showing the feedback circuit approach based on cloning the CymR repressor after the mCherry gene, both driven by the same (operated) promoter, P_{tec}. **F**) Plasmid map of the P_{tec}_cymR_P

variant. The exact DNA sequence between the mCherry STOP codon and the cymR ATG codon is shown. An additional RBS (the one used for the P_{23} promoter) was included to ensure translation of the downstream gene. **G**) Fluorescence intensity (left Y axis) and OD_{600nm} values (right Y axis) of the P_{tec}_cymR_P variant when induced at different starting OD_{600nm} (0.3, 0.1 and 0.01) for 15 hours (n = 3, mean ± SD, gain = 85).

Thermally aided switching for improving fold change

From previous experience, we were aware that the strength of many promoters in *L. plantarum* are temperature dependent (Dey, Blanch-Asensio et al. 2023). Similarly, we observed that the P_{tec} promoter is two-fold stronger at 37°C compared to 30°C (**Figure S4**). Furthermore, temperature also affects the growth rate of bacteria with typically slower growth at lower temperatures. Based on these, we speculated that temperature could influence the performance of the cumate genetic switch by offering lower leakiness at 30ºC and strong induced protein production at 37°C. We termed this concept as "*thermally aided switching*", involving both temperature and cumate to regulate the performance of the switch (**Figure 3A**).

We first evaluated the influence of temperature on the P_{23}_cymR variant through flow cytometry to confirm that the responses to temperature and cumate occurred across the entire population. Cultures prepared at a bacterial density of 0.01 OD_{600nm} were induced with 5 µM of cumate and incubated at both 30 and 37°C for 8 hours. Results showed low leakiness of the switch at 30°C without induction, and prominent levels of mCherry expression at 37°C (**Figure 3B**). Besides, induction at 30°C also worked very efficiently, with the entire population switching to higher levels of fluorescence intensity. Thermally aided switching was even visible in the coloration of the bacterial pellets (**Figure 3B**), which increased with both higher temperature and cumate induction.

We then estimated the kinetic performance of the genetic switch at both temperatures with and without cumate. The P_{23}_cymR variant exhibited a considerable delay in the start of leaky expression when grown at 30°C (>12 hours) instead of 37°C (>8 hours) while maintaining notable induced expression in the presence of cumate by these timepoints (**Figure 3C**). These timepoints corresponded to a higher bacterial density towards the end of the log-phase at 30°C (~1 OD_{600nm}) compared to 37°C (~0.8 OD_{600nm}) (**Figure 3C** and **2D**). This suggested that at 30°C, leakiness is suppressed till a slightly higher biomass compared to 37°C, although induced protein production at 30°C is lower. Accordingly, after 10 hours of induction, we calculated an 80-fold difference between uninduced and induced states at 30°C, and a 100-fold difference between the uninduced state at 30°C and induced state at 37°C (**Figure 3D**). We also evaluated the thermally aided switching

response for the P_{tec}_cymR_P variant since it was able to achieve higher levels of overall production. Once again, we detected a delay in the start of leaky expression when bacteria were grown at 30°C (>10 hours) compared to 37°C (>6 hours) (**Figure 3E** and **2D**). These time points also corresponded to a higher bacterial density at 30°C (~0.8 OD_{600nm}) than at 37°C (~0.6 OD_{600nm}) (**Figure 3E** and **2D**). At 10 hours, with this variant, we calculated a cumate-driven 72-fold increase in expression at 30°C, and a remarkable 215-fold increase in expression at 37°C with cumate compared to 30°C without cumate (**Figure 3F**). This was due to the considerably higher levels of induced protein production supported by the P_{tec}_cymR_P variant.

Beyond protein production, their secretion is also of great importance for industrial and medical applications since it allows for easier protein purification and programming bacteria to exert extracellular bioactivity (Reed and Chen 2013, Bai, Li et al. 2018, Neef, van Dijl et al. 2021).Thus, we proceeded to test the performance of the cumate switch on protein secretion. For this, we used NucA, a nuclease from *Staphylococcus aureus* that is commonly used in *L. plantarum* and other gram-positive bacteria such as *Lactococcus lactis* as a reporter protein for secretion since there is a simple assay to measure its activity (Le Loir, Nouaille et al. 2001, Nouaille, Morello et al. 2006, Mathiesen, Sveen et al. 2009). The assay is based on the degradation of fluorescently labeled DNA by NucA. Using this method, we previously reported that the Lp_3050 signal peptide to be highly efficient for secreting NucA with the P_{tec} promoter (Tadimarri, Blanch-Asensio et al. 2025). Accordingly, we cloned the Lp_3050_NucA gene under control of the cumate genetic switch, generating the P_{23}_cymR_NucA variant.

Based on the results with the mCherry expression, we expected that at 30°C without cumate, there would be low levels of NucA secretion whereas at 37 ºC with cumate, secretion of NucA would be higher (**Figure 3G**). We evaluated the thermally aided switching in both DNase agar and media, which contained fluorescently labeled DNA. In the agar experiment, 10 µL of induced and uninduced bacteria grown at both 30ºC and 37ºC were spotted on DNase agar and incubated at 37ºC for roughly 40 hours. We could not discern a halo around the spotted area of bacteria grown at 30ºC without cumate. On the other hand, there were clearly visible dark halo for the other three conditions, with the darkest and widest ones for the bacteria grown at 37ºC with and without cumate (**Figure 3H** and **S5A**). These results indicate that at 37ºC, the cumate genetic switch is also leaky for NucA, which matches with the results obtained with mCherry. Image analysis of the fluorescence intensity drop in the halo revealed that, at 37ºC, the halo was slightly daker with cumate than the one without (**Figure S5B**). For better quantification, the bacteria were grown and induced in the same way but then transferred into liquid DNase media with or without cumate and incubated at either 30ºC or 37ºC. After 24 hours, the

fluorescence of the media was measured, and the drop in fluorescence was correlated with a standard curve to estimate the concentration of secreted NucA. At 30ºC without cumate, NucA levels were below the detection limit, while over 1 nM of cumate was secreted from the bacteria with cumate. At 37ºC, roughly 9 and 11 nM were detected in the absence and presence of cumate respectively (**Figure 3I**).

Overall, the results with both mCherry and NucA proved that thermally aided switching with both cumate and temperature change can be an efficient approach to tightly regulate gene expression in *L. plantarum* when grown in culture.

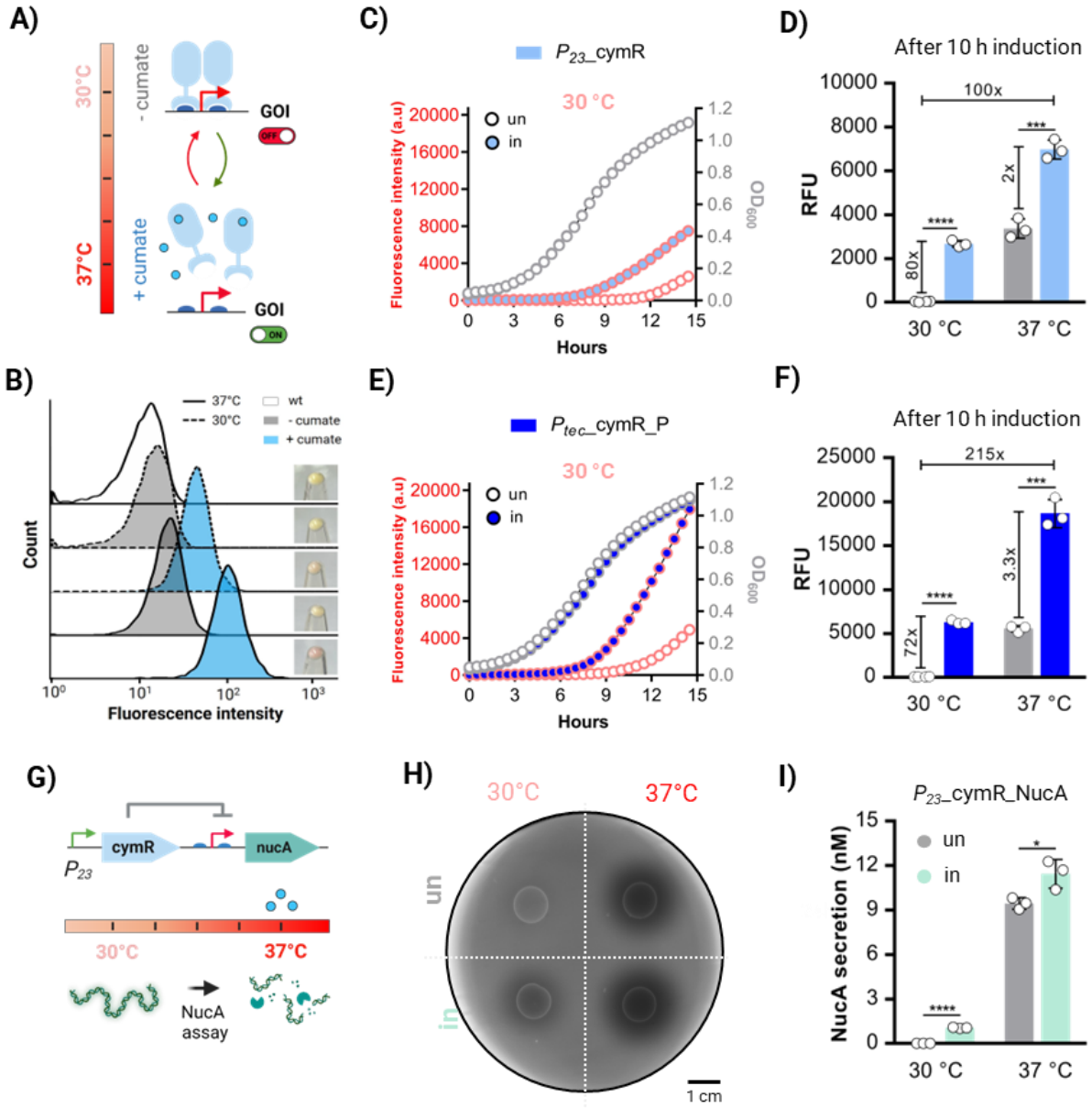

Figure 3: **Thermally aided switching.** **A)** Scheme depicting the thermally aided switching strategy involving both temperature and cumate. Proper turning on of the gene is achieved via both the incubation at 37°C and addition of cumate. **B)** Histograms showing the fluorescence intensity (after 8 hours) of the P_{23}_cymR variant at 30 and 37°and with and without addition of cumate. Bacterial pellets are shown on the right of each condition. **C)** Fluorescence intensity (left Y axis) and OD_{600nm} values (right Y axis) of the P_{23}_cymR variant when induced at 30°C for 15 hours (n = 3, mean ± SD). **D**) RFU values corresponding to hour 10 after induction for the P_{23}_cymR variant when induced at 37°C and 30°C (n = 3, mean ± SD). **E)** Fluorescence intensity (left Y axis) and OD_{600nm} values (right Y axis) of the P_{tec}_cymR_P variant when induced at 30°C for 15 hours (n = 3, mean ± SD). **F**) RFU values corresponding to hour 10 after induction for the P_{tec}_cymR_P variant when induced at 37°C and 30°C (n = 3, mean ± SD). **G**) Scheme depicting the cumate genetic switch controlling NucA expression. In the presence of cumate and at 37°C, maximized NucA production is achieved, which can be quantified via the NucA assay. **H**) 10 µL of P_{23}_cymR_NucA bacteria, uninduced and induced for 8 hours in MRS media at both 30 and 37°C, were spotted in a DNase agar plate and incubated at 37°C for 40 hours. **I**) Amounts of NucA secreted (in nM) by P_{23}_cymR_NucA bacteria after growing in DNase media for 24 hours at both 30 and 37°C and in the presence and absence of cumate (n = 3, mean ± SD).

Encapsulation-enhanced genetic switches

In our previously reported alginate core-shell encapsulation format for genetically engineered *L. plantarum* (PEARL) (Tadimarri, Blanch-Asensio et al. 2025), we observed steady protein production and secretion for 14 days without outgrowth of the bacteria. The results from that study suggested that the encapsulated bacteria stopped growing after a day or two but remained metabolically active to produce and secrete P_{tec}-driven recombinant proteins at a rate corresponding to log-phase in liquid cultures. From the results of the current study suggesting the best performance of the cumate switch in early- to mid-log-phase, we speculated that encapsulation in the PEARL format could prolong this performance. Since cumate is a small-molecule inducer, it was expected to diffuse inside the PEARLs and activate protein production in the encapsulated bacteria (**Figure 4A**). After fabricating PEARLs with the P_{23}_cymR variant, cumate was added to the media surrounding them and fluorescence was measured over 3 days. The expression of mCherry in these induced PEARLs was detected after 4 hours, slowly increased till ~12 hours then rapidly increased till nearly 24 hours (**Figure 4B**). The initial slow increase in expression may be since bacterial metabolism simultaneously supported growth and mCherry production during this time. This is supported by our previously reported observation that *L. plantarum* growth in PEARLs plateaus around 12 hours (Tadimarri, Blanch-Asensio et al. 2025). Beyond this point, the metabolic resources in the bacteria are forced predominantly towards mCherry production. The slight drop in fluorescence

after 24 hours suggests a saturation of the expressed protein within the bacteria and possibly bacterial death due to it (**Figure 4B**). More striking was the observation that leaky mCherry expression in the uninduced PEARLs was only observed after 15 hours, increased a little until ~20 hours and plateaued beyond this timepoint. On calculating the fold change between the induced and uninduced PEARLs, the highest value was surprisingly observed at 10.5 hours (92.5x), possibly due to negligible leaky expression, and after 24 hours, it stabilized between 25-35x (**Figure 4C**). These results confirmed our hypothesis that encapsulation can help to reduce the leakiness of the cumate switch, probably by locking the bacteria in a metabolic state akin to the early log-phase in liquid cultures.
When comparing the behavior P_{23}_cymR with P_{tec}_cymR_P in the PEARL format, we found that both performed very similarly with P_{tec}_cymR_P being a bit leakier (**Figure S6A,B**). In comparison, the pSIP_409 variant in the PEARL format exhibited expectedly negligible levels of uninduced leaky expression and low levels of induced mCherry production - ~37 and ~50 times lower than the P_{23}_cymR and the P_{tec}_cymR_P variants, respectively (**Figure S6C**). Thus, encapsulation of the bacteria in alginate reduced leakiness of the genetic switches but did not improve protein production of the weaker switch.

Since the PEARL format supported stable switching of mCherry production, we proceeded with the encapsulation of the P_{23}_cymR_NucA variant to test switchable protein secretion. For this, we incubated the PEARLs in liquid DNase media and measured the fluorescence in the media over time (**Figure 4D**). We tested four different switching scenarios over 2 days in the absence and presence of cumate: i) OFF-OFF - PEARLs incubated in DNase media without cumate for 1 entire day, then washed with sterile Milli-Q water, followed by another entire day incubation with fresh DNase media without cumate. ii) OFF-ON - day 1 without cumate and day 2 with cumate. iii) ON-OFF - day 1 with cumate and day 2 without cumate. iv) ON-ON - day 1 with cumate and day 2 with cumate. The OFF-OFF scenario showed that the genetic switch remained in the OFF state on both days with no detectable NucA secretion (same as control), which means that encapsulation effectively prevented leaky expression (**Figure 4E i**). The OFF-ON scenario also worked well, with encapsulated bacteria being activated only on the second day upon addition of cumate in the fresh DNase media (**Figure 4E ii**). This finding is particularly interesting from the ELM perspective since it highlights that encapsulated bacteria could remain inactive for hours and then be activated on demand. However, in the ON-OFF scenario, while there was strong secretion on the first day, switching did not effectively occur on the second day. There was a slight decrease in the magnitude to which fluorescence in the DNase media dropped (53% and 38% drop in fluorescence compared to the control in the first and second day, correspondingly), but the inactivation was not as sharp as the activation in the OFF-ON scenario (**Figure 4E iii**). This could be due to

retention of cumate within the PEARLs, keeping the switch active, slow release of accumulated NucA from the alginate, or continued secretion of NucA that was already produced in the bacteria. Most likely, all three phenomena influenced this outcome. Nevertheless, the result indicates that encapsulation can prolong the ON state beyond the period when the inducer is present. This is desirable in scenarios like living therapeutics for prolonged drug release with a short activation signal. Finally, for the ON-ON scenario, as expected, we detected a strong drop in fluorescence for the first and second day as well, confirming that the presence of cumate in the media sustained NucA secretion from the bacteria even in the second day (**Figure 4E iv**). These results indicated the possibility to switch between different states in PEARLs, which is highly desirable for developing smart ELMs (Wang, Liu et al. 2022).

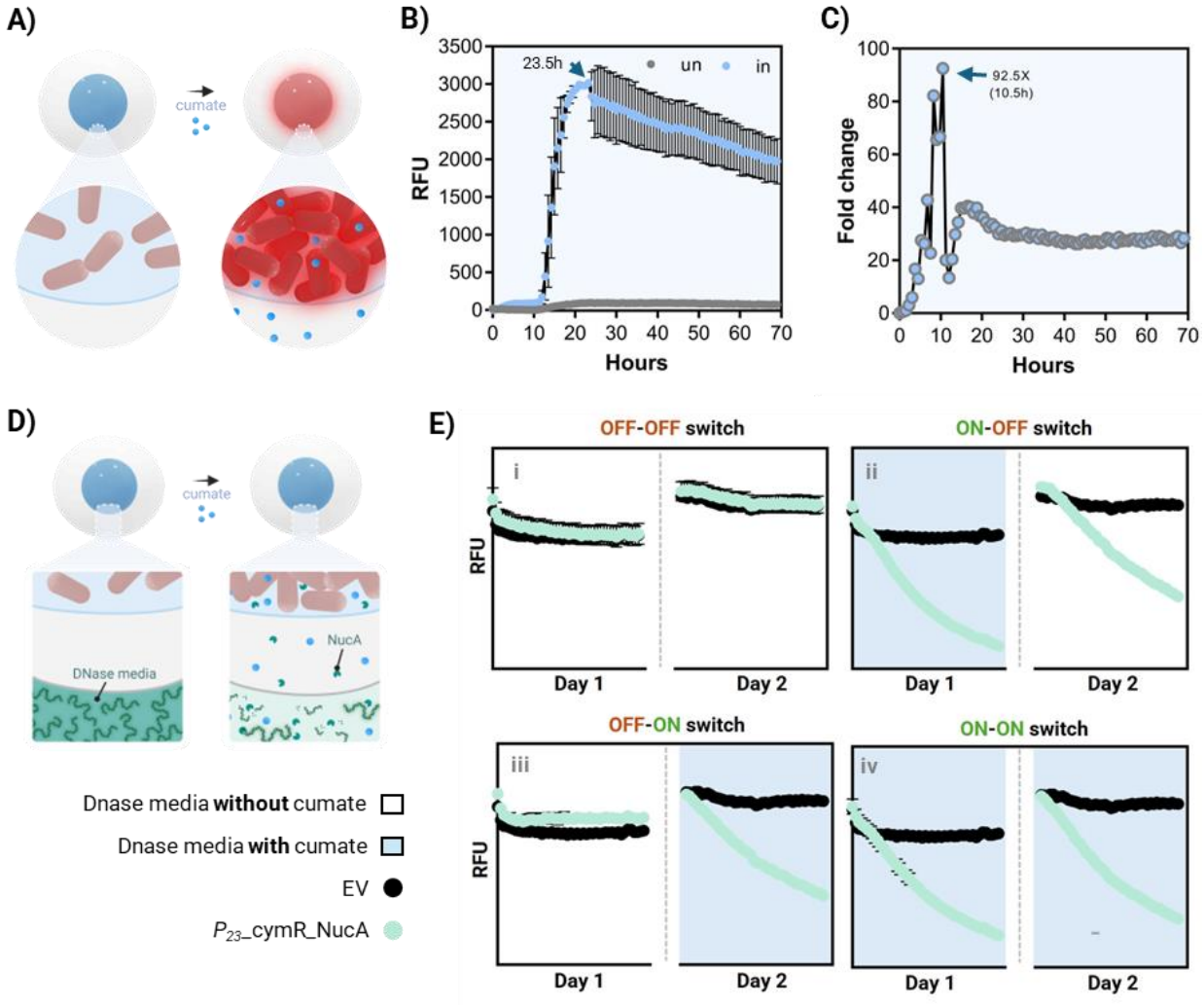

Figure 4: **Cumate genetic switch in PEARLs**. **A)** Scheme showing the induction of *L. plantarum* bacteria harboring the cumate switch when encapsulated in PEARLs. Upon induction, the core of the PEARLs turns red due to bacterial activation and subsequent mCherry intracellular production.

B) RFU for the P_{23}_cymR variant when encapsulated in PEARLs and incubated at 37°C for 70 hours (n = 3, mean ± SD). **C**) Fold changes for the induced state compared to the uninduced state for the P_{23}_cymR variant over 70 hours of growth at 37°C. **D)** Scheme showing the NucA production regulated by the cumate switch when bacteria are encapsulated in PEARLs. The cumate diffuses inside the core and activates the bacteria, which triggers the secretion of NucA into the shell. The diffusion of NucA into the DNase media results in the discoloration of the media due to NucA activity. **E**) P_{23}_cymR_NucA ON and OFF switches depending on the incubation of the PEARLs in DNase media with or without cumate on day 1 and in day 2. PEARLs were washed between days 1 and 2 and measurements are shown as RFUs (n = 4, mean ± SD).

Dual switchable PEARLs

Altogether, bacterial encapsulation within PEARLs enhanced the performance of the cumate switch by reducing the non-induced state leakiness while maintaining activity in the induced state. As we had correlated this to the bacteria being trapped in a growth phase that maintains uninduced repression of the P_{tec} promoter, we tested whether it would work for the highly leaky vanillate switch (**Figure 1C** and **S1B**). Accordingly, we observed a considerably enhanced performance of the vanillate switch when bacteria were encapsulated within PEARLs, with fold changes close to 15x after 20 hours of induction (**Figure 5A** and **5B**). These results were validated by fluorescence imaging, where red fluorescence was observed only in the cores of the induced PEARLs (**Figure S7A**). On the other hand, kinetic analysis of mCherry production in non-encapsulated bacteria with the vanillate switch yielded very poor fold changes that were consistently below 1.5x (**Figure S7B**). Thus, alginate bead encapsulation enhanced the performance of the vanillate switch by an order of magnitude.

Based on these promising results, we attempted co-encapsulation of the two *L. plantarum* strains engineered with cumate (P_{23}_cymR_NucA) and vanillate (P_{23}_vanR_mCherry) switches **(Figure 5C**). Encapsulation of bacteria in hydrogels offers the unique opportunity to establish stable co-cultures and thereby create multi-functional ELMs (Johnston, Yuan et al. 2020, Birnbaum, Manjula-Basavanna et al. 2021, Gilbert, Tang et al. 2021). The dual switchable PEARLs were induced individually with vanillate and cumate and with both inducers simultaneously. Fluorescence imaging revealed that only the PEARLs that were induced with vanillate showed detectable levels of mCherry expression (**Figure 5D**). In parallel, their NucA secretion was assessed by monitoring the drop in fluorescence in DNase media, which was observed only in the PEARLs induced with cumate (**Figure 5E**). Furthermore, both populations can also be induced simultaneously when both inducers are added to the media (**Figure 5D** and **5E**). This demonstrated that

multi-switching and multi-functional PEARLs can be created by encapsulating different engineered *L. plantarum* strains.

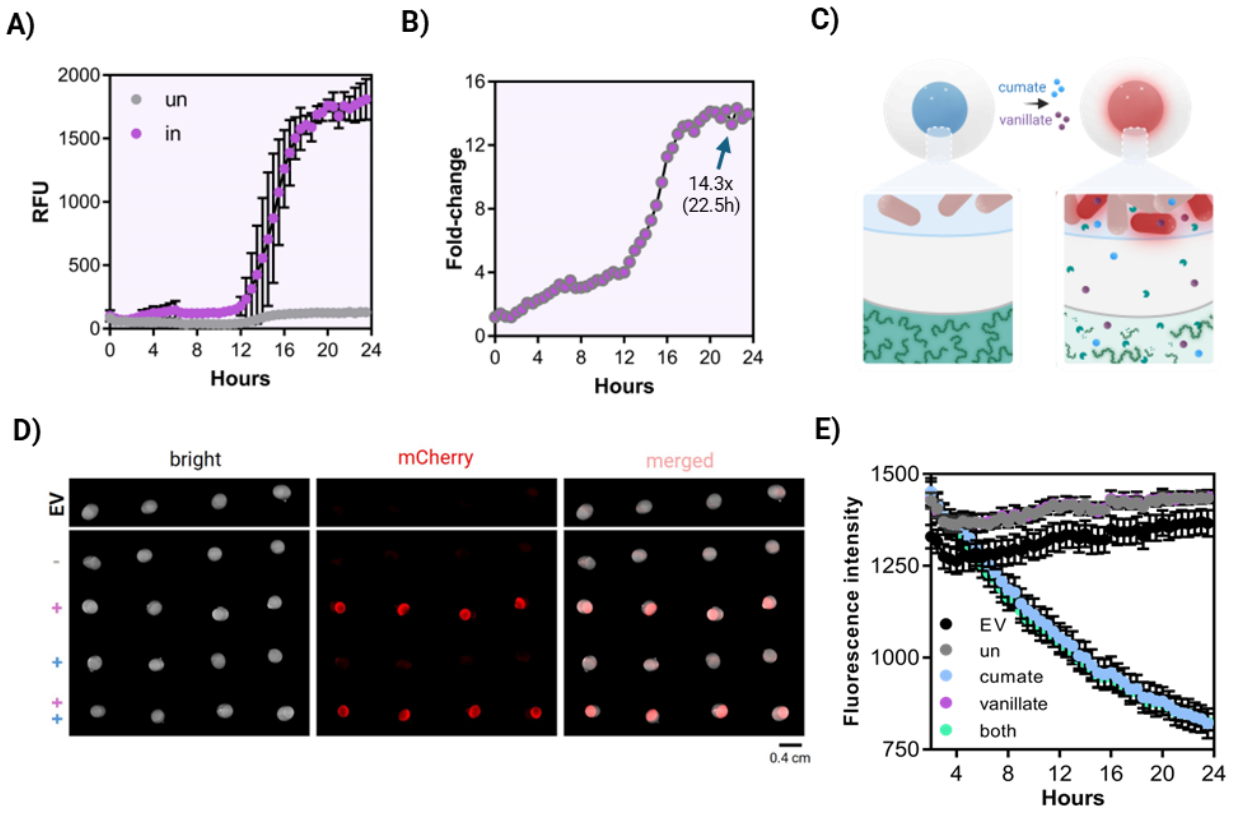

Figure 5: **Dual switchable PEARLs**. **A)** RFU values for the induced and uninduced states of the P_{23}_vanR variant when encapsulated in PEARLs and grown at 37°C for 23 hours (n = 4, mean ± SD). **B**) Fold-changes between the induced and uninduced states of the P_{23}_vanR variant when encapsulated in PEARLs and grown at 37°C for 23 hours. **C**) Scheme depicting the co-encapsulation of bacteria producing mCherry via the vanillate switch and secreting NucA via the cumate switch. Both inductions can be detected from the PEARLs by assessing the red fluorescence increase in the core of the PEARLs and the drop in the fluorescence in the DNase media surrounding the PEARLs. **D**) Red fluorescence captured from the PEARLs (P_{23}_cymR_NucA and P_{23}_vanR) that were incubated without any inducer, only with vanillate, only with cumate and with both inducers at 37°C for 24 hours. Empty Vector (the plasmid does not encode for any gene of interest) PEARLs were kept as negative control. Images were taken with the BioRad Gel Documentation System. **E**) Drop in fluorescence triggered by NucA secretion into the DNase media from the PEARLs. Empty Vector PEARLs were kept as negative control. (n = 4, mean ± SD).

Cumate genetic switch in micro-PEARLs

Encouraged by these results we proceeded to develop the PEARL system into a more compact format better suited for different applications. Furthermore, the PEARL format faces other limitations since it is a time-consuming manual approach that can lead to fabrication errors and has poor scalability. Therefore, we adopted a more automated, time-saving, up-scalable approach to produce a higher number of beads, with smaller sizes (Berninger, Mitter et al. 2016, Rojas-Muñoz, de Jesús Perea-Flores et al. 2024). For this, we used an electrospray microencapsulator B-390/B-395 (Buchi) to generate core-shell alginate micro-beads (micro-PEARLs) that ranged in sizes from 100 µm to 500 µm. In these micro-PEARLs, we encapsulated a single *L. plantarum* strain that constitutively produced a red fluorescent protein, mScarlet3, and secreted NucA (**Figure 6A**). Hence, we could simultaneously monitor gene expression within the micro-PEARLs by tracking red fluorescence production and assessing protein secretion through the DNase assay. After incubating the micro-PEARLs for 24 hours on a DNase agar plate, we could detect a prominent dark halo around the set of micro-PEARLs, and red fluorescence in their core. Furthermore, the halo increased in size after 5 days, suggesting continued secretion of NucA over time (**Figure 6B, S8A**). Moreover, bacterial growth within the cores could be observed even by eye after incubating the micro-PEARLs in 2-mL tubes with MRS media for 24 hours (**Figure 6C**).

Next, we evaluated if these micro-PEARLs could be induced upon addition of cumate in the media. For that, we used the P_{23}_cymR variant, which would ideally produce mCherry in the core of the micro-PEARLs when cumate is added to the media (**Figure 6D**). As expected, it was possible to track the induction over time with a clear increase in red fluorescence only in the presence of cumate (**Figure 6E**). Kinetic analysis over 24 hours clearly revealed that even in the micro-PEARLs format, encapsulation ensured almost completely uninduced repression of mCherry expression. This difference was even visible through macroscopic fluorescence imaging (**Figure 6F**). Microscopic analysis of the micro-PEARLs revealed mCherry fluorescence predominantly in the cores and only in those that were induced by cumate (**Figure 6G**, **S8B** and **S8C**). These results validate that the more automated, time-saving, effective, and compact encapsulation method for *L. plantarum* allows the bacteria to grow efficiently while maintaining them in an active and cumate-switchable state.

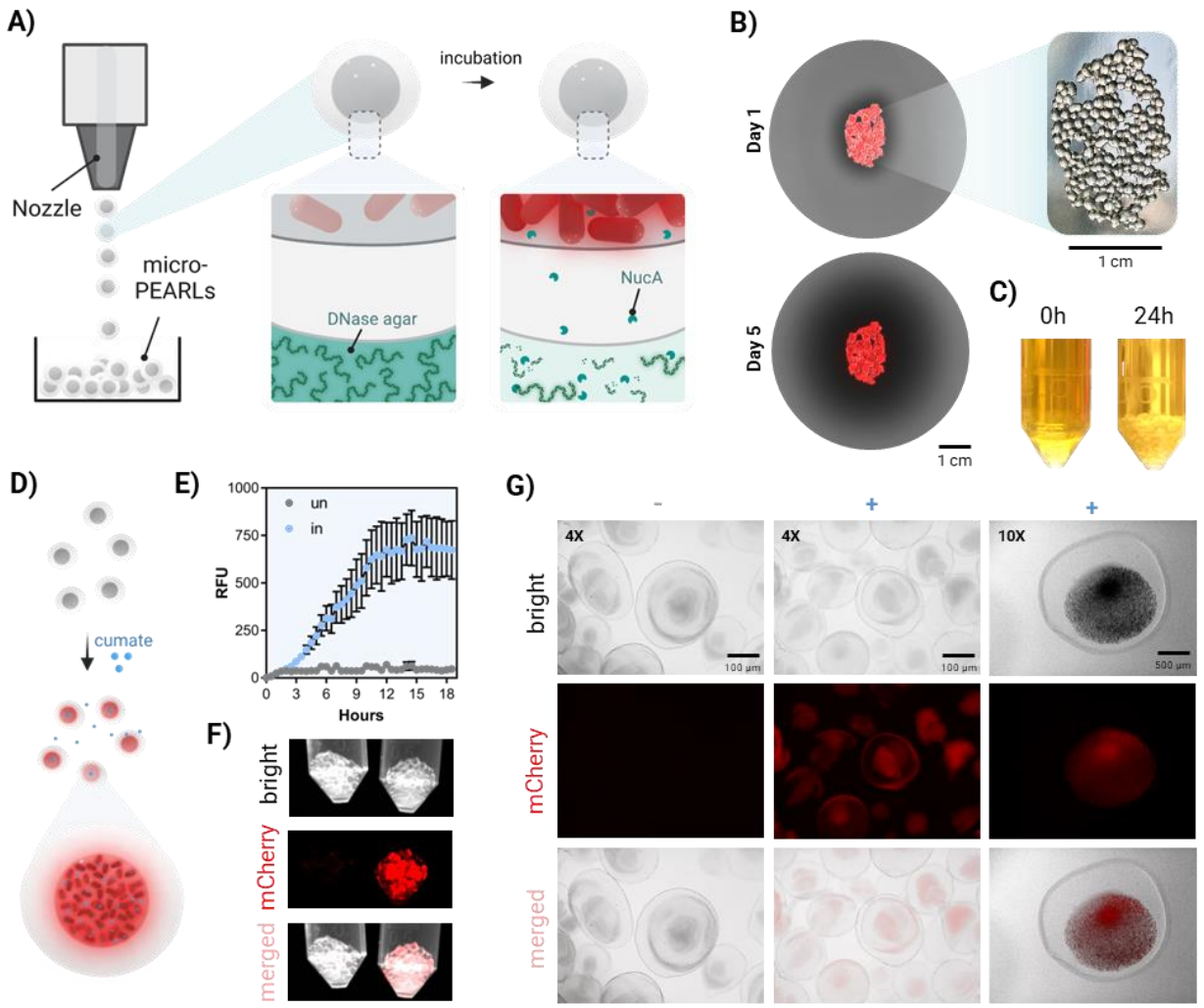

Figure 6: **Cumate switch in micro-PEARLs.** **A)** Scheme showing micro-PEARL fabrication with the microencapsulator. The micro-PEARLs contain bacteria that produce mScarlet3 and secretes NucA. After incubation, the core of the micro-PEARLs turns red, and the fluorescence of the DNase agar fades away due to degradation of fluorescently labelled DNA. **B)** DNase agar plates with micro-PEARLs after 1 and 5 days of incubation at 37°C. Images taken using the BioRad Gel Documentation System. **C)** 2 mL tubes with micro-PEARLs incubated in MRS media after 0 and 24 hours. The diameter of the 2-mL tube is 11 mm. **D)** Scheme of the cumate induction in micro-PEARLs. Upon induction, the core of the micro-PEARLs turns red due to mCherry intracellular production. **E**) RFU values of the P_{23}_cymR variant when encapsulated in micro-PEARLs and induced with cumate for 19 hours (n = 3, mean ± SD). **F**) BioRad Gel Documentation System images of induced and uninduced micro-PEALSs after 24 hours of incubation at 37 ºC. **G**) Microscopy images, at both 10X and 4X, of uninduced and induced micro-PEARLs after 24 hours of incubation at 37 ºC.

CONCLUSIONS

In this study, we have successfully modified *L. plantarum*'s strongest constitute promoter, P_{tec}, into a genetic switch responsive to cumate. However, the switch suffered from leakiness of gene expression associated with bacterial growth, especially when the bacteria entered the late log-phase. Due to the natural capacity of P_{tec} to be more active at higher temperatures, we explored a workaround to reduce the leakiness of the cumate switch through thermally aided switching, in which the uninduced state was maintained at 30ºC and cumate induction was performed at 37ºC. However, a much more promising strategy to ehance the performance of the switch was discovered through the encapsulation of the engineered bacteria in macroscopic alginate beads to form PEARLs. This surprisingly suppressed leaky expression of the cumate switch while supporting high levels of protein production and secretion. This effect extended beyond the cumate switch to the much leakier vanillate switch and even sustained the performance of both switches in a co-culture setting. Furthermore, the encapsulation-enhanced switching was not dependent on the size of the encapsulation matrix as the effect persisted even in micro-PEARLs, which can be rapidly produced in an automated manner. We hypothesize that encapsulation within alginate mechanically and metabolically restricts bacterial growth but maintains them in a metabolic state akin to the low log-phase in liquid cultures, since nutrients remain available in abundance. In this metabolic state, the repressor remains active and suppresses leaky expression.

These encapsulation-enhanced switches are promising for the development of responsive ELMs towards medical, environmental, and industrial applications (Harimoto, Hahn et al. 2022, Lyu, Huang et al. 2024, Altin-Yavuzarslan, Drake et al. 2025). By combining this effect with mechanically switchable smart materials, it may be possible to control the performance of such genetic switches by exerting *in situ* changed in the mechanical properties of the material. Nevertheless, further investigation is needed to understand the underlying mechanisms causing this effect and may reveal interesting insights into unique metabolic or biochemical regulation processes in lactobacilli.

SUPPORTING INFORMATION

Supporting information is available from the Wiley Online Library.

FUNDING

This work was supported by a Deutsche Forschungsgemeinschaft (DFG) Research grant (Project # 455063657), a DFG Collective Research Center (SFB1027) subproject grant (Project #200049484), and the Leibniz Association through the Leibniz Science Campus on Living Therapeutic Materials (LifeMat).

CONFLICT OF INTEREST

The authors declare no conflict of interest.

DATA AVAILABILITY

The raw and processed datasets along with relevant metadata are available from the corresponding author upon reasonable request.

ACKNOWLEDGEMENTS

We thank Prof. Geir Mathiesen (Norwegian University of Life Sciences) for sharing the pLp_3050sNuc plasmid (Addgene plasmid # 122030) with us. The *L. plantarum* WCFS1 strain was a kind gift from Prof. Gregor Fuhrmann (Friedrich-Alexander-Universität, Erlangen-Nürnberg). The authors used Biorender for the illustrations of this study. We thank the group of Prof. Wilfried Weber for granting access to their Buchi B-390 microencapsulator device for the fabircation of the micro-PEARLs and providing initial training for the device.

REFERENCES

Altin-Yavuzarslan, G., et al. (2025). "Genetically programmed engineered living materials as high-performance bioplastics." Matter **8**(1).

Bai, F., et al. (2018). "Bacterial type III secretion system as a protein delivery tool for a broad range of biomedical applications." Biotechnology Advances **36**(2): 482-493.

Berninger, T., et al. (2016). "The smaller, the better? The size effect of alginate beads carrying plant growth-promoting bacteria for seed coating." Journal of Microencapsulation **33**(2): 127-136.

Bina, X. R., et al. (2014). "Construction of a tetracycline inducible expression vector and characterization of its use in Vibrio cholerae." Plasmid **76**: 87-94.

Birnbaum, D. P., et al. (2021). "Hybrid Living Capsules Autonomously Produced by Engineered Bacteria." Advanced Science **8**(11): 2004699.

Blanch-Asensio, M., et al. (2023). "In vitro assembly of plasmid DNA for direct cloning in Lactiplantibacillus plantarum WCSF1." PLOS ONE **18**(2): e0281625.

Blanch-Asensio, M., et al. (2024). "Expanding the genetic programmability of Lactiplantibacillus plantarum." Microbial Biotechnology **17**(1): e14335.

Blanch-Asensio, M., et al. (2024). "Discovery of a high-performance phage-derived promoter/repressor system for probiotic lactobacillus engineering." Microbial Cell Factories **23**(1): 42.

Brautaset, T., et al. (2009). "Positively regulated bacterial expression systems." Microbial Biotechnology **2**(1): 15-30.

Daniel, R., et al. (2013). "Synthetic analog computation in living cells." Nature **497**(7451): 619-623.

Dey, S., et al. (2023). "Novel genetic modules encoding high-level antibiotic-free protein expression in probiotic lactobacilli." Microbial Biotechnology **16**(6): 1264-1276.

Gilbert, C., et al. (2021). "Living materials with programmable functionalities grown from engineered microbial co-cultures." Nature Materials **20**(5): 691-700.

Giraffa, G., et al. (2010). "Importance of lactobacilli in food and feed biotechnology." Research in Microbiology **161**(6): 480-487.

Halbmayr, E., et al. (2008). "High-Level Expression of Recombinant β-Galactosidases in Lactobacillus plantarum and Lactobacillus sakei Using a Sakacin P-Based Expression System." Journal of Agricultural and Food Chemistry **56**(12): 4710-4719.

Harimoto, T., et al. (2022). "A programmable encapsulation system improves delivery of therapeutic bacteria in mice." Nature Biotechnology **40**(8): 1259-1269.

Heiss, S., et al. (2016). "Evaluation of novel inducible promoter/repressor systems for recombinant protein expression in Lactobacillus plantarum." Microbial Cell Factories **15**(1): 50.

Johnston, T. G., et al. (2020). "Compartmentalized microbes and co-cultures in hydrogels for on-demand bioproduction and preservation." Nature Communications **11**(1): 563.

Karlskås, I. L., et al. (2014). "Heterologous Protein Secretion in Lactobacilli with Modified pSIP Vectors." PLOS ONE **9**(3): e91125.

Klotz, A., et al. (2023). "A Synthetic Cumate-Inducible Promoter for Graded and Homogenous Gene Expression in Pseudomonas aeruginosa." Applied and Environmental Microbiology **89**(6): e00211-00223.

Kunjapur, A. M. and K. L. J. Prather (2019). "Development of a Vanillate Biosensor for the Vanillin Biosynthesis Pathway in E. coli." ACS Synthetic Biology **8**(9): 1958-1967.

Le Loir, Y., et al. (2001). "Signal Peptide and Propeptide Optimization for Heterologous Protein Secretion in Lactococcus lactis." Applied and Environmental Microbiology **67**(9): 4119-4127.

Lutz, R. and H. Bujard (1997). "Independent and Tight Regulation of Transcriptional Units in Escherichia Coli Via the LacR/O, the TetR/O and AraC/I1-I2 Regulatory Elements." Nucleic Acids Research **25**(6): 1203-1210.

Lyu, Y., et al. (2024). "Macroencapsulated bacteria for in vivo sensing and therapeutics." Matter **7**(4): 1440-1465.

Mao, J., et al. (2024). "Relieving metabolic burden to improve robustness and bioproduction by industrial microorganisms." Biotechnology Advances **74**: 108401.

Martínez-Fernández, J. A., et al. (2019). "Bile-induced promoters for gene expression in Lactobacillus strains." Applied Microbiology and Biotechnology **103**(9): 3819-3827.

Mathiesen, G., et al. (2009). "Genome-wide analysis of signal peptide functionality in Lactobacillus plantarum WCFS1." BMC Genomics **10**(1): 425.

Meng, Q., et al. (2021). "Optimization of Electrotransformation Parameters and Engineered Promoters for Lactobacillus plantarum from Wine." ACS Synthetic Biology **10**(7): 1728-1738.

Meyer, A. J., et al. (2019). "Escherichia coli “Marionette” strains with 12 highly optimized small-molecule sensors." Nature Chemical Biology **15**(2): 196-204.

Monachese, M., et al. (2012). "Bioremediation and Tolerance of Humans to Heavy Metals through Microbial Processes: a Potential Role for Probiotics?" Applied and Environmental Microbiology **78**(18): 6397-6404.

Neef, J., et al. (2021). "Recombinant protein secretion by Bacillus subtilis and Lactococcus lactis: pathways, applications, and innovation potential." Essays in Biochemistry **65**(2): 187-195.

Nguyen, T.-T., et al. (2011). "Quantitative transcript analysis of the inducible expression system pSIP: comparison of the overexpression of Lactobacillus spp. β-galactosidases in Lactobacillus plantarum." Microbial Cell Factories **10**(1): 46.

Nouaille, S., et al. (2006). "Complementation of the Lactococcus lactis Secretion Machinery with Bacillus subtilis SecDF Improves Secretion of Staphylococcal Nuclease." Applied and Environmental Microbiology **72**(3): 2272-2279.

Pan, N., et al. (2021). "Oral Delivery of Novel Recombinant Lactobacillus Elicit High Protection against Staphylococcus aureus Pulmonary and Skin Infections." Vaccines **9**(9): 984.

Peirotén, Á. and J. M. Landete (2020). "Natural and engineered promoters for gene expression in Lactobacillus species." Applied Microbiology and Biotechnology **104**(9): 3797-3805.

Reed, B. and R. Chen (2013). "Biotechnological applications of bacterial protein secretion: from therapeutics to biofuel production." Research in Microbiology **164**(6): 675-682.

Rojas-Muñoz, Y. V., et al. (2024) Probiotic Encapsulation: Bead Design Improves Bacterial Performance during In Vitro Digestion (Part 2: Operational Conditions of Vibrational Technology). Polymers **16**, DOI: 10.3390/polym16172492

Rud, I., et al. (2006). "A synthetic promoter library for constitutive gene expression in Lactobacillus plantarum." Microbiology **152**(4): 1011-1019.

Santos Rocha, C., et al. (2012). "Anti-inflammatory Properties of Dairy Lactobacilli." Inflammatory Bowel Diseases **18**(4): 657-666.

Scheppler, L., et al. (2002). "Recombinant Lactobacillus johnsonii as a mucosal vaccine delivery vehicle." Vaccine **20**(23): 2913-2920.

Seo, S.-O. and C. Schmidt-Dannert (2019). "Development of a synthetic cumate-inducible gene expression system for Bacillus." Applied Microbiology and Biotechnology **103**(1): 303-313.

Sørvig, E., et al. (2005). "High-level, inducible gene expression in Lactobacillus sakei and Lactobacillus plantarum using versatile expression vectors." Microbiology **151**(7): 2439-2449.

Tadimarri, V. S., et al. (2025). "PEARL: Protein Eluting Alginate with Recombinant Lactobacilli." Small **n/a**(n/a): 2408316.

Tan, C., et al. (2009). "Emergent bistability by a growth-modulating positive feedback circuit." Nature Chemical Biology **5**(11): 842-848.

Wang, J., et al. (2012). "Selection of potential probiotic lactobacilli for cholesterol-lowering properties and their effect on cholesterol metabolism in rats fed a high-lipid diet." Journal of Dairy Science **95**(4): 1645-1654.

Wang, Y., et al. (2022). "Engineered living materials (ELMs) design: From function allocation to dynamic behavior modulation." Current Opinion in Chemical Biology **70**: 102188.

Yang, W.-T., et al. (2018). "Immune response characterization of mice immunized with Lactobacillus plantarum expressing spike antigen of transmissible gastroenteritis virus." Applied Microbiology and Biotechnology **102**(19): 8307-8318.

Yoon, S., et al. (2024). "Development of high-performance inducible and secretory expression vector and host system for enhanced recombinant protein production." Scientific Reports **14**(1): 30780.

Zhang, L., et al. (2022). "Development and Application of Two Inducible Expression Systems for Streptococcus suis." Microbiology Spectrum **10**(4): e00363-00322.

Zhang, Z., et al. (2018). "Roles and applications of probiotic Lactobacillus strains." Applied Microbiology and Biotechnology **102**(19): 8135-8143.

Zhang, Z., et al. "Advancements in Lactiplantibacillus plantarum: probiotic characteristics, gene editing technologies and applications." Critical Reviews in Food Science and Nutrition: 1-22.